IEEE Access
Multidisciplinary | Rapid Review | Open Access Journal

Received 22 January 2025, accepted 17 March 2025, date of publication 24 March 2025, date of current version 31 March 2025.

Digital Object Identifier 10.1109/ACCESS.2025.3554140

RESEARCH ARTICLE

Fuzzy Rule-Based Combination Model for the Fire Pixel Segmentation

ALBERTO LOPEZ-ALANIS[1], HECTOR DE-LA-TORRE-GUTIERREZ[1], ARTURO HERNÁNDEZ-AGUIRRE[2], AND MARÍA T. ORVAÑANOS-GUERRERO[3]

[1]Center for Research in Mathematics, Aguascalientes 20200, Mexico
[2]Department of Computer Science, Center for Research in Mathematics (CIMAT), Guanajuato 36023, Mexico
[3]Facultad de Ingeniería, Universidad Panamericana, Aguascalientes 20296, Mexico

Corresponding author: Hector de-la-Torre-Gutierrez (hector.delatorre@cimat.mx)

The work of Alberto Lopez-Alanis was supported by Secihti through the Postdoctoral Scholarship under Grant 718822.

ABSTRACT Color-feature-based wildfire pixel segmentation has become a challenging task extensively addressed in various research studies. Rule-based models aim to identify fire pixels in a binary manner by determining whether the pixel intensity exceeds a specified threshold value. The authors determine the thresholds by analyzing diverse collections of images that contain wildfires. This has resulted in a lack of consensus on the thresholds determined by various researchers, even when the same color space is used during the examination process. Additionally, determining fire pixels in a binary manner complicates the handling of uncertainty and vagueness in color information. This research aims to enhance fire-pixel segmentation by integrating color-based rule models with a fuzzy set approach, which effectively addresses uncertainty and vagueness. The proposed approach automatically learns the optimal set of fuzzy operators and rules for fire detection to construct a combined model. To address the limitations of combining binary class labels, this approach modifies the rule form proposed by various authors to obtain a fuzzy set of data, such as a grayscale fire map, instead of a crisp set of data, such as a binary fire map. In addition, our proposal uses a genetic algorithm approach to construct the best combination model. The final binary form of the fire map is calculated using the widely used Otsu method. The presented method is evaluated qualitatively and quantitatively in a well-accepted dataset designed for wildfire pixel segmentation tasks. The model obtained outperforms state-of-the-art rules and traditional strategies for combining binary labels in the F-measure and IoU metrics.

INDEX TERMS Fire-pixel segmentation, fuzzy rules, genetic algorithm, color-based rule model, combination model.

I. INTRODUCTION

Wildfires are natural disasters that significantly affect ecosystems, the economy, and society [1]. Due to global warming, the patterns of wildfires have changed [2], making early detection crucial. Traditionally, ground crew inspections have been the most common method for fire detection [3]. However, this approach is unreliable because of its limitations in area coverage and detection speed.

Several techniques [3] have been developed to address these limitations for the early detection of wildfires. Advanced technologies now incorporate computer vision techniques [4], which play a key role in improving the response time of firefighting teams and minimizing the damage caused by wildfires [5]. Various fire detection methods have been designed for image classification to determine the presence or absence of fire in images. However, some researchers have proposed methods to detect fire pixels using segmentation techniques. This research work focuses on fire-pixel segmentation.

Regardless of the fire pixel segmentation approach, the authors have proposed to tailor a forest fire detection model by considering the most relevant fire characteristics. Among the features used to construct fire models, we can mention

The associate editor coordinating the review of this manuscript and approving it for publication was Frederico Guimarães.

color, texture, edges, and, in the case of video sequence analysis, flame flicker, and flame motion [6]. Often, the proposed approaches utilize color as the main feature to develop fire detection models. Moreover, some researchers proposed the use of various color representations to improve forest fire detection or segmentation [7]. Fire detection can be performed using both video sequences and static images; however, most methods involve an analysis based on color features. The literature identifies two types of fire detection color-based approaches: rule-based and machine- or deep learning-based. In this study, our aim is to tackle the fire pixel segmentation task in a rule-based fire color model approach.

Celik et al. [8] utilized the color of statistics to characterize fire pixels. Five rules were proposed using the RGB color space. The mean value in the red channel and six thresholds comprise the rules. The thresholds are determined by analyzing a set of images that contain fire pixels. The model proposed by Huang et al. [9], combines color information from two color spaces; RGB and HSI. Specifically, three rules were developed: two rules concerning the RGB color space and one rule using the saturation channel from HSI color space in combination with the red channel. Decision thresholds are determined by various experiments using images that contain fire pixels. The authors claim that using the saturation channel allows for discrimination in brightness variations, avoiding misclassifying background and foreground.

Töreyin et al. [10], calculated the color distribution of fire pixels from sample images that contain fire scenes. Gaussian mixture was computed in the RGB color space. The threshold is determined by two standard deviations of the computed Gaussian distributions. Vipin [11] constructs a set of rules for fire pixel classification using RGB and YC_rC_b color spaces. The authors claim that using a color space that decouples luminance from chrominance improves fire pixel detection. The authors proposed seven rules: two using the RGB color space and five based on chromatic information from the YC_rC_b color space.

Rule-based models rely on the researcher's expertise to determine the threshold for pixel classification. Hence, various authors have proposed guided learning approaches. Philips et al. [12], proposed a supervised learning approach. A 3D histogram in RGB color space is constructed to calculate the probability that a pixel is a fire pixel. The determination of the flame pixel is expressed as an inequality in which the probability has to be greater than a threshold value k. Chino et al. [13], utilized Naive Bayesian to learn a fire model. The YC_rC_b color space was used to avoid luminance variations. Additionally, the authors proposed characterizing the flame using LBP uniform patterns. Maheen and Aneesh [14], calculate a feature extraction stage to segment the image, then calculate a color correlogram in conjunction with the Naive Bayesian classifier. Typically, the performance of rule-based models depends on the knowledge embedded in the rules by experts. In other words, different knowledge results in different performance. In addition, the performance of rule-based models varies because they utilize different color spaces and analyze diverse sets of images.

Recently, various deep learning approaches have been proposed to address the shortcomings in the classification tasks of rule-based models [15]. Frizzi et al. [16], proposed a convolutional neural network (CNN) to detect the fire pixel. The authors claim that they used a classical architecture of nine convolutional layers and Max pooling. In addition, the image is processed in the RGB color space using the kernel size 3×3. Zhao et al. [17], proposed a deep convolutional neural network (DCNN) named Fire_Net in combination with a saliency detection method for fast fire detection. The DCNN consists of 15 layers, 8 of which are for convolution and 4 of which are for max-pooling. Then, the following 3 layers capture complex co-occurrence statistics. Jadon et al. [18] developed a CNN designed to achieve real-time performance. The named FireNet network consists of 14 layers. The authors utilized the Rectified Linear Unit (Relu) and Softmax as activation functions. FireNetv2 was developed by Shees et al. [19] as an improvement on their predecessor. The size of the model decreased due to the number of computations required and the number of parameters needed to set up the network. Despite deep learning approaches achieving reliable performance in fire pixel detection, neural networks operate as a closed-box, making it challenging for humans to comprehend the computations of the fire detection model [20], [21].

In this work, we propose an aggregation model for fire pixel segmentation to enhance the performance of rule-based fire color models while maintaining interpretability for human understanding. In computer vision, various authors focus on developing a structural understanding of image content using segmentation approaches. As a result, segmentation plays a crucial role in various computer vision tasks to understand images [22]. Lang et al. [23], proposed a method to leverage the base learner to identify the confusable regions in query images and further refine the predictions of the meta-learner. This author also proposed a scheme called BAM [24] to alleviate the bias problem in FSS models. It utilizes the base learner to identify the confusable (base) regions in the query image or point cloud and subsequently refines the predictions made by the meta-learner. Lang et al. [22] also introduced a flexible and generic framework incorporating a novel self-reasoning scheme to derive support-induced proxies, effectively addressing the typical challenges associated with few-shot segmentation (FSS) tasks. This framework was specifically designed to mitigate confusion and improve discriminatory capabilities. Cheng et al. [25] proposed a few-shot segmentation approach called Holistic Prototype Activation (HPA). This method introduces two key modules: the prototype activation module and the cross-referenced decoder, aimed at addressing the issues of overfitting to base category targets and the generation of inaccurate segmentation boundaries, respectively.

In addition, segmentation has been used in other computer vision tasks, such as medical image segmentation [26], robotic perception, image compression [27], and salient object segmentation [28], among others.

As mentioned above, rule-based fire models exhibit varying performance; different rules perform differently in the fire pixel segmentation task. In this study, our objective is to improve the performance of rule-based models by aggregating multiple fire pixel detection rules. An aggregation model combines multiple pieces of information to make a decision aimed at addressing a specific task [29]. Diverse aggregation approaches have been proposed to address various computer vision tasks such as visual saliency detection [30], [31], gesture recognition [32], and image classification [33], among others.

To the best of our knowledge, there are not enough studies on aggregation proposals to enhance fire pixel segmentation. In the research work of Buza et al. [34], the authors systematically experimented with combining color-based fire detection rules for pixel-wise classification. The authors used the simple *"and"* operator in all their experiments to combine the binary labels generated by the rules. First, the authors evaluated all the rules to identify the best rule. The authors proposed combining the Top-1 rule with other rules that achieved a minimum F-measure of 0.3 while excluding rules that performed poorly. Specifically, the authors performed the combinations in pairs, combining the Top-1 rule with each rule that met the minimum score condition. In addition, Buza carried out another experiment that combined the rules based on the color space used in their design. The combination was performed using rules that utilize RGB, YC_bC_r, CIELAB, and HWB color spaces. The simple aggregation function used in their experiments has barely improved fire pixel segmentation. The proposed aggregation approach considers the binary outcome computed by the rules, constraining the handling of ambiguity and uncertainty in the data.

The proposed approach aims to improve the segmentation of the fire pixel using an aggregation model while maintaining human interpretability. In pursuit of this goal, the proposed approach utilizes fuzzy logic operators to obtain a readable model. Fuzzy logic theory has previously been used to address diverse tasks in various research works. Soni and Mehta [35] integrated a fuzzy logic controller and fuzzy clustering for the diagnosis and prognosis of incipient faults in power transformers, incorporating critical parameters such as dissolved gas analysis, moisture content, furans, interfacial tension, and degree of polymerization, among others. Kaur et al. [36] proposed a novel clustering approach based on a fuzzy concept to segment medical images, demonstrating that it performs better compared to other methods. Yin and Hadjiloucas [37] discussed fuzzy rule-based filters, including cellular automata, vector filters, and deep learning classifiers, comparing their performance with conventional methods. Key advantages include effective noise suppression, edge preservation, and computational efficiency.

In summary, our method aims to construct a fuzzy rule-based aggregation model to enhance fire pixel segmentation. The proposed system takes advantage of the knowledge of various rule-based models designed in different color spaces. In contrast to binary label aggregation techniques, our proposal handles uncertainty using a fuzzy set approach to associate a degree of membership with the fire pixel class. Our proposal is as follows. Firstly, our proposed system utilizes a modified form of the rules as input. Specifically, we modified the rules to generate a gray-level fire map instead of a binary image. We use the rules proposed in the research work of Anh et al. [38], Prema et al. [39], Buza and Akagic [7], and Dzigal et al. [40]. Secondly, unlike binary label combination techniques, our system employs fuzzy operators for the combination, allowing us to handle imprecision and vagueness in fire pixel detection. Third, we employ a genetic algorithm to determine the optimal set of rules for fire-pixel segmentation to minimize reliance on human experts for rule design.

The remainder of this document is organized as follows. First, we present the methodology and details of the proposal in Section II. In Section III, we provide details of the parameters, dataset, and evaluation protocol used in our test series. The results of our experiments are given in Section IV. Section V presents the conclusion and future research directions.

II. METHODOLOGY

In this section, we provide the theoretical background of our proposal. In Figure 1, we show the overview of the proposed method. Since we aim to exploit different rule-based fire detection models by merging their rules, our proposed system is three-fold: 1) In Figure 1(a), we depict the stage for generating an aggregation model. First, our proposal computes the feature maps used as input for our learning stage. The feature maps are calculated using a modified form of the rules of various state-of-the-art fire detection methods. The rules were modified to allow our system to find the best combination in a continuous range of values instead of fusing binary labels. Then, our proposal explores the combinations of rules by using fuzzy operators. Specifically, we used a genetic algorithm approach to find the best rule-based model to aggregate fire detection rules. Our system performs N experiments and retrieves the best model computed on each experiment. 2) In Figure 1(b), the N best models of each experiment are evaluated using a subset of the dataset. The best model assessed in this partition of the dataset is selected to be evaluated in the test stage. 3) In Figure 1(c), the test stage is performed using the best model generated in the learning step. Our aggregation model performs fire detection by calculating the features and computing the fuzzy rules found in the learning stage for a new incoming image.

The rest of this section is organized as follows. Firstly, we establish the fundamental principles for effectively combining the outcomes of various fire rules. Secondly,

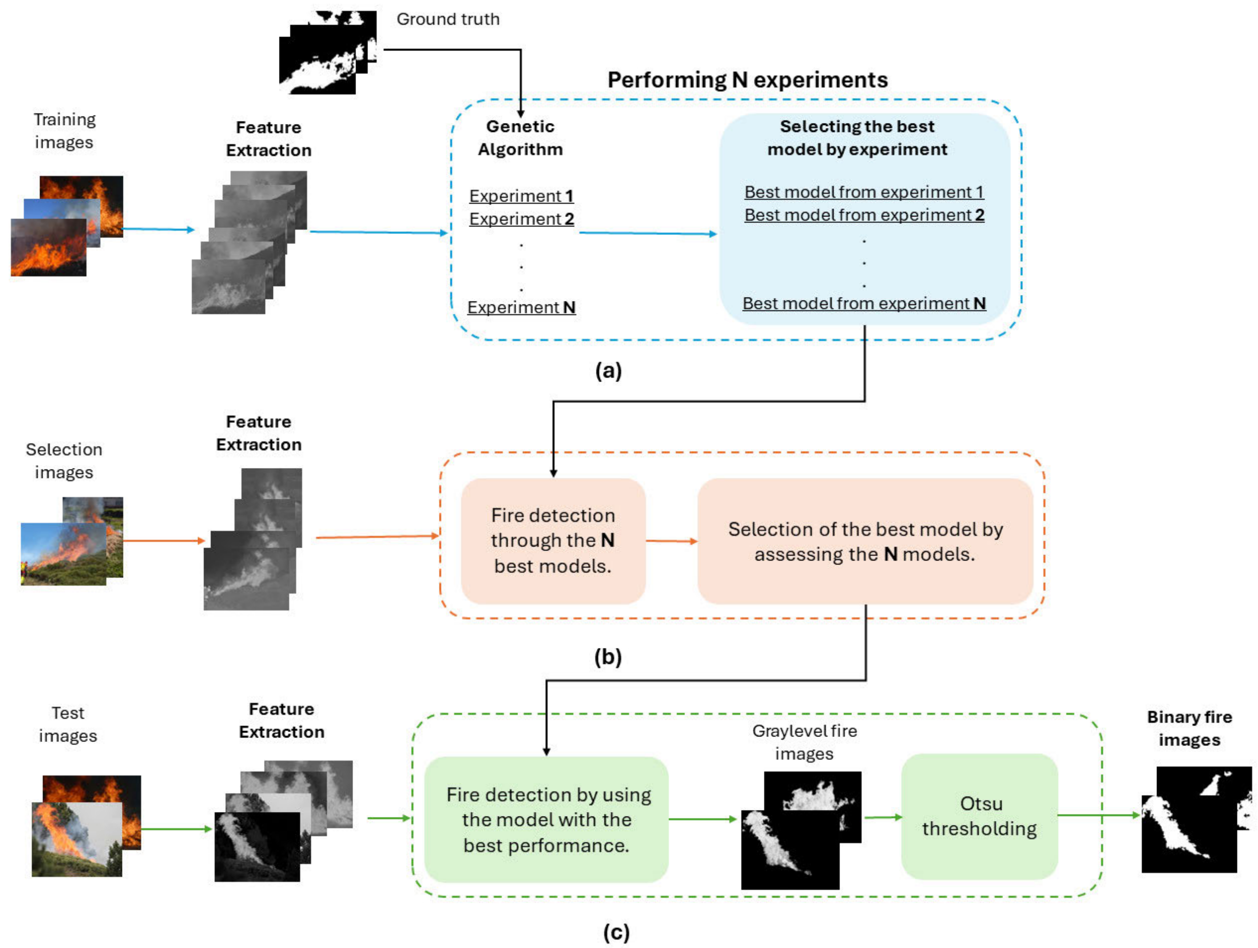

FIGURE 1. **Overview of proposed approach. We conducted 30 experiments to validate our proposed approach. (a) First, the proposal computes the feature extraction stage using the training image subset.Second, the system searches for the optimal combination of rules using a genetic algorithm and fuzzy operators.Third, our system selects the best model from each experiment. (b) The proposal evaluates the best models using a subset of validation images to select the highest scoring model. (c) The proposed model computes fire pixel segmentation on an input image.**

we present the foundations of the genetic algorithm. Third, we present the theoretical background of fuzzy theory for combining fire detection rules. In addition, we give details of the aggregation operators utilized. Finally, we introduce the rule-based models proposed by various authors for fire detection. In addition, we introduce the modified form of the rules used as inputs to our system.

A. THE AGGREGATION OF FIRE DETECTION RULES

The combination of results from various classifiers has proven to be reliable in addressing various binary segmentation tasks on image processing [41]. The combination of outcomes from various segmentation approaches aims to improve the classification regardless of the semantic segmentation task [42]. In this research, our aim is to combine the results from the fire pixel detection rules to improve fire-pixel segmentation.

Consider $R = \{r_1, r_2, \ldots, r_L\}$ the set of L fire detection rules. Then, we fuse the outputs of the L fire detection rules using Equation 1,

$$\widehat{r} = F(r_1(x), r_2(x), \ldots, r_L(x)), \tag{1}$$

where F is a combination rule and the output $r_i(x)$ is the determination of the pixels as fire or not fire.

We propose using genetic algorithms to find the combination function F and to encode the combination rule in a tree structure. Since we aim to enhance fire pixel segmentation, selecting the objective function is not trivial. For improving fire pixel segmentation, the objective function can be any conventional function that aims to assess segmentation. Then, depending on the selection of the assessing function, the proposed approach maximizes or minimizes the objective function. In our experiments, we use the Matthews correlation coefficient (MCC) as our objective function given in Equation 2,

$$MAX\ MCC(\widehat{r}) = \frac{(F_1 \times F_2) - (F_3 \times F_4)}{(F_1+F_3)\times(F_1+F_4)\times(F_2+F_3)\times(F_2+F_4)}, \tag{2}$$

where MAX is the maximize function, $F_1 = TP(\widehat{r})$ true positive, $F_2 = TN(\widehat{r})$ true negative, $F_3 = FP(\widehat{r})$ false positive and $F_4 = FN(\widehat{r})$ false negative.

B. GENETIC APPROACH

Genetic algorithms (GA) are useful in machine learning and optimization tasks [43]. GA has been used to adjust rule-based classifiers, that is, to evolve rules [44] using principles of natural evolution to guide the exploration of plausible solutions [45]. In the field of computer vision research, GA has been used in various tasks such as feature selection [46], [47], optimization [48], [49], and computer vision algorithms [50], [51], among others.

GAs encode candidate solutions in generic structures called chromosomes S [52]. Then, the tuning is about the rules, functions, and terminals. In our approach, we used a tree structure to encode candidate solutions and to tune the rules that determine the sequence of combinations encoded in an individual. The semi-guided stochastic search process assesses a candidate solution through an objective function named the fitness function J. In our proposed system, our fitness function is the straightforward classification score [53].

Five essential stages comprise the implementation of GAs [54]: 1) The initial population refers to the generation of a set of individuals $\pi = \{S_1, S_2, \ldots, S_n\}$, encoding candidate solutions. The fitness solution $J(S)$ assesses each solution; the higher the score, the better the candidate solution. 2) Mating stage, a set M of individuals is selected from π to be crossovering. Different bases have been proposed for the design of the M set. The roulette wheel uses a proportional probability distribution to the fitness function to set the odds of an individual being selected; the better the score, the higher the probability of being selected. 3) Crossover: A fixed number of individuals are selected from the M set to form a set of parent couples M_P. Each couple of parents produces two new individuals to build the set of offsprings O. The crossover operation can be performed in various manners. Our approach performs a crossover by swapping the entire branch from the tree structures utilized to represent the candidate solutions. 4) At the mutation stage, a small probability is assigned to determine whether an individual is selected to be modified. The alteration occurs by modifying a small portion of the individual. In our proposal, the mutation occurs by modifying just one node or branch. 5) Selection consists of choosing the individuals that survive to the next generation (iteration), the selection is composed of the set π and O. The most popular method of selecting the next population set is the elitism strategy, which involves keeping the best individuals. We adopted this selection strategy.

C. FUZZY SET THEORY FOR FIRE DETECTION

The fuzzy set theory introduced by Zadhe [55], is a useful mathematical tool for handling imprecision and approximate reasoning [56]. A fuzzy set A in a finite nonempty set X, called universe, is characterized by a membership function of A [57]. The definition of the membership function is given in Equation 3,

$$\mu_A : X \rightarrow [0, 1], \tag{3}$$

where μ_A is the membership function that assigns a degree of association of $x \in X$ to the fuzzy set A. An element x with a membership of 1 is considered to belong completely to the fuzzy set A. In contrast, an element x with a membership of 0 is considered not to belong to the fuzzy set A. The intermediate values are given to the elements that are not certain to belong to the set A. Due to their ability to handle uncertainty, fuzzy sets have been used in various image processing algorithms. Among fuzzy-based image processing tasks, we can mention low-level processes such as clustering [58], [59], and image compression [60], among others.

As mentioned earlier, our objective is to aggregate various rules for fire detection. The fire detection rules we can find in the literature, are composed of inequalities and relational operators that, in conjunction, determine in a binary manner if a pixel in an image corresponds to the fire class or corresponds to the background. We modify the rule form given by various authors to aggregate rules-based models using fuzzy sets. The modified form assigns a pixel value in the $[0 - 1]$ range. Typically, the membership function that defines information from the image is the gray-level intensity value. In our approach, the element x is the pixel image and the membership function μ_A is the pixel intensity value. That is, a fire pixel has a membership of 1, and a background pixel has a membership of 0. The intermediate values are given to the pixels that are uncertain of classifying as fire or background.

Since we modified the rules to obtain the output mapping in the range $[0 - 1]$ instead of obtaining the binary form proposed by the authors, the combination of rules is performed using a set of aggregation functions for fuzzy sets widely studied and used in various academic and research works, such as [29], [54], [56], [61], [62], and [63].

In our proposal, the operator nodes are the fuzzy aggregation functions. In fuzzy set theory, the intersection of two sets is performed by the t-norm functions. In contrast, the union of two fuzzy sets is performed by the t-conorm functions. The t-norm and the t-conorm functions are defined as the minimum and maximum value among two elements of a fuzzy set [62], respectively.

We can find various definitions of the functions t-norm and the t-conorm in the literature. Specifically, we implement the minimum, product, bounded difference t-norm functions. Regarding the t-conorm we utilized the maximum, probabilistic sum, and bounded sum functions. In Table 1, we give the t-norm and t-conorm functions definition proposed to be used in our rule-based aggregation model.

In addition, we include the Lukasiewicz and Kleen-Dienes fuzzy set operations. The Lukasiewicz and Kleen-Dienes

TABLE 1. Summary of maximum and minimum fuzzy operators utilized for our proposal, where A and B are fuzzy sets.

Function	Type	ID Operator
$min\{A, B\}$	Minimum	mi
AB	Product	tn
$max\{0, A + B - 1\}$	Bounded difference	co
$max\{A, B\}$	Maximum	ma
$A + B - AB$	Probabilistic sum	tc
$min\{1, A + B\}$	Bounded sum	di

operators are categorized as fuzzy implication operators. These operators are fundamental in the construction of fuzzy rule-based systems to correctly handle fuzzy conditions of the form "*if p then q*" [64]. In Table 2, we present a summary of the fuzzy implication operators.

TABLE 2. Summary of fuzzy implication operators, where A and B are fuzzy sets.

Function	Type	ID Operator
$min\{1, 1 - A + B\}$	Lukasiewicz	lk
$max\{1 - A, B\}$	Klen-Dienes	kd

Since intersections and unions (maximum and minimum) are insufficient to aggregate fuzzy sets [54], we include a variety of functions that aim to fill values between maximum and minimum. Specifically, we utilized operators such as mean operators and symmetric sum operators. Table 3 presents the operators utilized in our implementation.

TABLE 3. Summary of fuzzy mean and symmetric sums operators.

Function	Type	ID operator
$\sqrt{AB}$	Geometric mean	gm
$\frac{2AB}{A+B}$	Harmonic mean	hm
$\frac{A+B-AB}{1+A+B-2AB}$	Symmetric sum	nn
$\frac{AB}{1-A-B+2AB}$	Symmetric sum	as

D. FEATURE EXTRACTION

The proposed aggregation approach utilizes various rule-based fire detection methods as input. Rule-based methods are made up of inequalities that are rules of the form *if* (*antecedent*) *then* (*consequence*). The methods combine the inequalities using Boolean operators to construct the model fire detection.

Generally, the combination of the models is performed using the binary label computed by the models. Our approach aims to aggregate the knowledge of various fire detection models to improve their performance. In contrast to binary-label aggregation approaches, our method utilizes a modified form of the rule proposed in other methods. In Equation 4, we give the traditional form of the rule.

$$if\ (condition)\ then\ (fire\ label), \tag{4}$$

where the *condition* is defined by a relational operator such as $<$, $>$, $=$ or any other combination of this operators i.e.

$$condition = (Left\ operand)\ >\ (Rigth\ operand), \tag{5}$$

Equation 5, is an example of the most common condition proposed in various fire detection algorithms. The operands can be intensity pixel values or threshold values in a given color space.

To allow our approach to exploit the color information of each state-of-the-art rule, we proposed to represent the rule so that our proposal can find the best combination of rules in a continuous range variable instead of in a binary-label manner. The modified rule allows us to combine knowledge from various fire detection paradigms and assign a degree of association with the fire class. The general form of the modified rule is given in Equation 6, where instead of giving a label after evaluating an inequality, we calculate the arithmetical difference among the left and right operands of the inequality;

$$condition = (Left\ operand)\ -\ (Rigth\ operand). \tag{6}$$

Specifically, we utilize four state-of-the-art approaches as inputs for our proposed aggregation approach. We utilize the model proposed by Anh et al. [38], which uses two color spaces: the RGB and YC_rC_b. In addition, we use the rules proposed in the YC_rC_b color space by Prema et al. [39]. Also, we use the rules designed by Buza and Akagic [7] constructed in the RGB color space. Similarly, we utilize the rules presented by Dzigal et al. [40]; the rules were designed in the HSV, HSL, and HWB color spaces.

1) YC_BC_R-RGB COLOR MODEL (NGUYEN ET AL.)

Anh et al. [38], utilized two color spaces that code the color information under different basis. The RGB color space was used to determine the relationship of intensity values of fire pixels. They found that the R and G channels contain higher intensity than channel B. The rule in which they expressed this relationship is presented in equation 7,

$$Rule_1 = if\ (R\ >\ G\ >\ B)\ then\ (Fire\ Pixel). \tag{7}$$

Furthermore, they claimed that the fire-pixel color represented in the RGB color space depends on the specific channel. That is, they established the relation that the fire pixel presents in the rule expressed in equation 8,

$$Rule_2 = if\ (R > R_{th})\ \wedge\ (G\ >\ G_{th})\ \wedge\ (B > B_{th})\ then\ (Fire\ Pixel), \tag{8}$$

where $R_{th} = 190$, $G_{th} = 100$, and $B_{th} = 140$. The authors empirically determined the threshold values.

On the other hand, they proposed to utilize the YC_bC_r color space to extract brightness information from the scene. The rule designed by the researchers is given in the equation 9,

$$Rule_3 = if\ (Y \geq C_r) \wedge (C_r \geq C_b)\ then\ (Fire\ Pixel). \tag{9}$$

The authors found that the values of the fire pixels are more significant in the channels Y, C_b, and C_r than their mean values. The proposed rule is given in equation 10,

$$Rule_4 = if\ (Y \geq \mu_Y) \wedge (C_r \geq \mu_{C_r}) \wedge (C_b \geq \mu_{C_b})\ then\ (Fire\ Pixel), \tag{10}$$

where the μ_Y, μ_{C_r}, μ_{C_b} are the mean of Y, C_r, and C_b channels. The joint of the four rules comprises the rule-based color model for fire detection.

The modified form of the rules in equations 7 - 10 is given in equations 11 - 20,

$$r_1 = R - G, \tag{11}$$
$$r_2 = G - B, \tag{12}$$
$$r_3 = R - R_{th}, \tag{13}$$
$$r_4 = G - G_{th}, \tag{14}$$
$$r_5 = B_{th} - B, \tag{15}$$
$$r_6 = Y - C_r, \tag{16}$$
$$r_7 = C_r - C_b, \tag{17}$$
$$r_8 = Y - \mu_Y, \tag{18}$$
$$r_9 = C_r - \mu_{C_r}, \tag{19}$$
$$r_{10} = \mu_{C_b} - C_b, \tag{20}$$

2) YC_BC_R COLOR MODEL (PREMA ET AL.)

In the research work of Prema et al. [39], the authors proposed to use YC_bC_r color space to handle luminance separated from chrominance. They claim that this color space exhibits a reliable performance even when illumination variations in the background occur. The model proposed by Prema is composed of two rules. The rules were designed using separated chrominance components Y, C_b, and C_r.

The authors observed that the C_r component has higher values for fire pixels than the C_b component. In addition, they claim that fire pixels present a higher value in the Y component than in the C_b component. The rule-based color model was designed taking into account the observation mentioned above. We present the rules designed by the authors in equations 21 and 22,

$$Rule_5 = if\ (Y > C_b \wedge C_r > C_b)\ then\ (Fire\ Pixel), \tag{21}$$

$$Rule_6 = if\ \left| C_b - C_r \right| > T\ then\ (Fire\ Pixel), \tag{22}$$

where $T = 80$ was chosen by the authors. The authors proposed to utilize the conjunction operator to combine the two rules. To utilize the rules in our proposal, we modified the form of the rule in 21 as given in equations 23 and 24,

$$r_{11} = Y - C_b, \tag{23}$$
$$r_{12} = C_r - C_b. \tag{24}$$

The rule in equation 22 is modified as in equation 25,

$$r_{13} = \left| C_b - C_b) \right| - T. \tag{25}$$

3) RGB COLOR MODEL (BUZA ET AL.)

Buza and Akagic [7] presented a fire detection model based on the RGB color space. The color model is embedded into an unsupervised algorithm for the determination of the region of interest. Nevertheless, we utilize the rule-based color model, avoiding the post-processing presented by the authors. First, the authors calculated the geometric mean of each color channel R, G, and B. Then, they calculated a new RGB color image $I'_{[R,G,B]}$ by computing the new pixel intensity using equation 26,

$$I'_{[R,G,B]} \leftarrow [R - \mu_R, G - \mu_G, B - \mu_B], \tag{26}$$

where μ_R, μ_G, μ_B are the geometric mean of the R, G, and B channels, respectively. Then, I' is used to obtain a mask that represents the candidates as fire pixels. The fire pixels are determined using equation 27,

$$Rule_7 = \begin{cases} if\ (I'_{[R]} < I'_{[B]})\ then\ (No\ Fire\ Pixel), \\ if\ ((I'_{[R]} + I'_{[B]}) < I'_{[G]})\ then\ (No\ Fire\ Pixel), \\ otherwise\ (FirePixel). \end{cases} \tag{27}$$

To utilize the rules as input for our proposal, we consider the preprocessing equation in 26 as a rule, then modify the rule form of equation 26, and give the new rule form in equations 28, 29, and 30.

$$r_{14} = I'_{[R]} - \mu_R, \tag{28}$$
$$r_{15} = I'_{[G]} - \mu_G, \tag{29}$$
$$r_{16} = I'_{[B]} - \mu_B. \tag{30}$$

The rule given in equation 27 was modified in the form presented in equations 31 and 32,

$$r_{17} = I'_{[R]} - I'_{[B]}, \tag{31}$$
$$r_{18} = (I'_{[R]} + I'_{[B]}) - I'_{[G]}. \tag{32}$$

4) HSV-HSL-HWB COLOR MODEL (DZIGAL ET AL.)

A hybrid model was proposed by Dzigal et al. [40], exploiting the combination of different color components of various color spaces. Specifically, they utilized the HSV, HSL, and HWB color spaces, which are color representations that separate chromatic information from brightness variations. The authors calculated the mean values of the components S, W, and B. Dzigal established the relationship between the color channels and the mean and threshold values. The rules

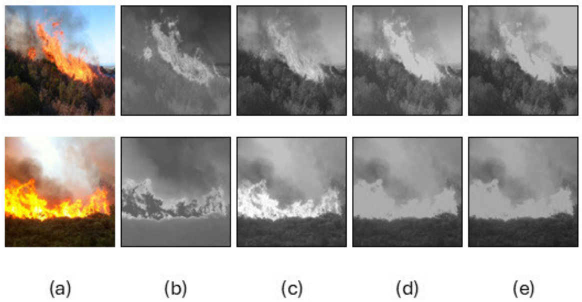

FIGURE 2. Samples out of the features used as input to our system. (a) Input image. (b) Sample of results from Nguyen's rules. (c) Sample of results from Prema's rules. (d) Sample of results from Buza's rules. (e) Sample of results from Dzigal's rules.

constructed by the authors and the relational condition are given in Equation 33,

$$if\ (Rule_8\ \wedge\ Rule_9\ \wedge\ Rule_{10}\ \vee\ Rule_{11}\ \vee Rule_{12}\ \vee\ Rule_{13})\ then\ (Fire\ Pixel). \tag{33}$$

where the definitions of the rules are given in Equation 34,

$$\begin{aligned} Rule_8 &= (S > 35)\\ Rule_9 &= (H \geq 330\ \wedge\ H \leq 65)\\ Rule_{10} &= (L > 70)\\ Rule_{11} &= (B < \mu_B\ \wedge\ W < \mu_W)\\ Rule_{12} &= (W > \mu_W \wedge\ S > \mu_S)\\ Rule_{13} &= (W \geq\ 98\ \wedge\ B \leq\ 2) \end{aligned} \tag{34}$$

The modified forms of the rules are presented in Equation 35,

$$\begin{aligned} r_{19} &= S - 35,\\ r_{20} &= 65 - H,\\ r_{21} &= H - 330,\\ r_{22} &= L - 70,\\ r_{23} &= \mu_B - B,\\ r_{24} &= \mu_W - W,\\ r_{25} &= W - \mu_W,\\ r_{26} &= S - \mu_S,\\ r_{27} &= W - 98,\\ r_{28} &= 2 - B, \end{aligned} \tag{35}$$

It should be mentioned that the H channel is mapped in the range $[0° - 360°]$ and the W and B channels are mapped in the range $[0\% - 100\%]$.

Finally, in Table 4, we summarize the rules of the four methods used to aggregate. The rules presented in Table 4 are the modified form utilized as inputs of our fuzzy rule-based aggregation system.

In Figure 2, we present samples from the results obtained by computing individual fire detection rules. The images are calculated in grayscale.

TABLE 4. Summary of rules utilized as inputs of our proposal.

Rule used as input for our proposal	Author
$r_1 = R\ -\ G$	Nguyen
$r_2 = G\ -\ B$	Nguyen
$r_3 = R\ -\ R_{th}$	Nguyen
$r_4 = G\ -\ G_{th}$	Nguyen
$r_5 = B_{th}\ -\ B$	Nguyen
$r_6 = Y\ -\ C_r$	Nguyen
$r_7 = C_r\ -\ C_b$	Nguyen
$r_8 = Y\ -\ \mu_Y$	Nguyen
$r_9 = C_r\ -\ \mu_{C_r}$	Nguyen
$r_{10} = \mu_{C_b}\ -\ C_b$	Nguyen
$r_{11} = Y\ -\ C_b$	Prema
$r_{12} = C_r\ -\ C_b$	Prema
$r_{13} = \lvert C_b\ -\ C_b) \rvert\ -\ T$	Prema
$r_{14} = I'_{[R]} - \mu_R$	Buza
$r_{15} = I'_{[G]} - \mu_G$	Buza
$r_{16} = I'_{[B]} - \mu_B$	Buza
$r_{17} = I'_{[R]} - I'_{[B]}$	Buza
$r_{18} = (I'_{[R]} + I'_{[B]}) - I'_{[G]}$	Buza
$r_{19} = S - 35$	Dizigal
$r_{20} = 65 - H$	Dizigal
$r_{21} = H - 330$	Dizigal
$r_{22} = L - 70$	Dizigal
$r_{23} = \mu_B - B$	Dizigal
$r_{24} = \mu_W - W$	Dizigal
$r_{25} = W - \mu_W$	Dizigal
$r_{26} = S - \mu_S$	Dizigal
$r_{27} = W - 98$	Dizigal
$r_{28} = 2 - B$	Dizigal

III. EXPERIMENT SETUP AND PARAMETERS

In this section, we present the parameters used to carry out our series of tests. First, we introduce the datasets used in our experiments. Second, we give the metrics used to assess the performance of the state-of-the-art methods and our proposal. Third, we give the setup parameters utilized by our evolutionary approach and provide examples of the evolution performed by our proposal and the model obtained. Fourth, we present an analysis of the constructed combination model. Finally, we present the evaluation protocol used to conduct our test series.

A. DATASETS

We used the CORSICAN [65] fire dataset (CFDB) to evaluate the proposed approach and state-of-the-art methods. The CORSICAN dataset has been used in various research works on fire segmentation [66]. The images are available online on request. The dataset consists of 500 images of wildfires in the visible spectrum, 100 images of multimodality, and five sequences of 30 images of multimodality of wildfires. The authors provide a binary ground truth in which the fire pixels are annotated as white pixels and the background as black pixels. The authors also describe the color information of the fire pixels; they realize that the fire color pixels are orange, white-yellow, and red. The diversity of wildfire images containing complex background contexts, the heterogeneity of fire-color pixels, and the presence of distractors such as fire-color objects make fire segmentation challenging. In Figure 3, we present examples of images from the dataset.

FIGURE 3. Examples of CORSICAN dataset and their pixel annotations. First row, color images. Second row, ground truth images.

The distribution in channel H of the fire color is represented in Figure 4. We compute a histogram to determine the color distribution of the fire pixels. We construct the histogram using the conversion of the color space to HSV. Specifically, we used the H channel to prevent our analysis from being biased by illumination variations. The histogram shows that the chromatic content is mostly represented in channel H's low-level range. Hence, we use the H channel to extract valuable information about the distribution of fire color.

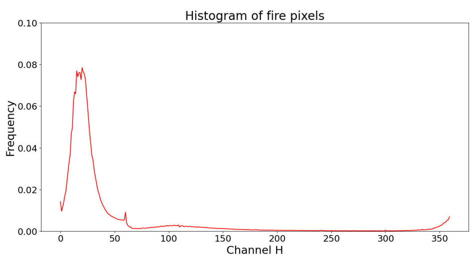

FIGURE 4. Histogram of the fire pixels. We use the H channel to construct the histogram, avoiding illumination affectations.

In Table 5, we present the color distribution of the fire pixels. We utilized quartiles to describe the chromaticity information. We can notice that the color content is predominantly in Q_1, Q_2, and Q_3. In addition, the intensity values of 50% and 75% of the population are in the lower range of channel H. This can be because the fire color is decoded in the lower range of the H channel in the HSV color space. Recalling that the H channel is circular, the chromatic content is decoded in a complete revolution from 0 ° to 360 ° degrees; the fire color is also decoded close to the completion of the revolution of the H color channel. The 25% of the population is above the Q_3 quartile.

On the other hand, in Table 6, we present the statistical information on the fire size of the dataset. We calculated the area of the image and the area of the fire in the image; the area was calculated in pixel units. The data in the table show that most of the images contain a small fire area. The 75% of the image population contains a small fire area, at most 28.02% of the image area.

TABLE 5. Distribution of the fire color in the channel H. We use the quartiles to describe the fire pixels.

Quartile	Intensity in the H channel
$Q_1(25\%)$	15
$Q_2(50\%)$	22
$Q_3(75\%)$	35

TABLE 6. Area of the fire on the images. We use quartiles to describe the percentage of fire area in the images within the dataset.

Quartile	Area of fire
$Q_1(25\%)$	9.28 %
$Q_2(50\%)$	17.54 %
$Q_3(75\%)$	28.02 %

In general, the CORSICAN dataset is an appropriate dataset for assessing fire detection models. The diverse condition of illumination is a task that any fire detection model must tackle. Furthermore, the heterogeneous fire content in the CORSICAN dataset makes it challenging to test the generalization capabilities of any fire model.

B. METRICS

The methods are evaluated quantitatively using the entries in the confusion matrix, such as True Positive (TP), True Negative (TN), False Positive (FP), and False Negative (FN). Specifically, we compare the methods using the F-measure, the weighted average of the Precision and Recall metrics.

The equations used to calculate the precision, recall, and F measures are presented in Eqs. (36), (37), and (38) respectively.

$$precision = \frac{TP}{(TP + FP)}, \tag{36}$$

$$recall = \frac{TP}{(TP + FN)}. \tag{37}$$

$$F\_measure = \frac{(\beta^2 + 1) \times precision \times recall}{\beta^2 \times precision + recall}, \tag{38}$$

where we set $\beta = 1$.

Additionally, we evaluated the performance of the diverse approaches by using the Jaccard index (IoU), as shown in Eq. (39):

$$IoU = \frac{TP}{TP + FP + FN}. \tag{39}$$

The IoU index measures the overlap between the ground truth and the predicted segmentation [67].

C. EVALUATION PROTOCOL

We qualitatively and quantitatively compare our system's performance to the other state-of-the-art methods to assess our proposal. The qualitative evaluation is two-fold. First, we compare the output images obtained from our approach with the output images computed by the individual rules. Second, we compare the images computed by the state-of-the-art fire detection methods and the images calculated by our proposal.

On the other hand, the quantitative evaluation is performed as follows: 1) First, we evaluate our results and the results computed from the individual rules presented previously ($Rule_{1-13}$). That is, we computed a fire map from each rule proposed by the authors. 2) Second, we evaluate the results of fully implementing fire detection methods and our proposal. Specifically, we utilize the Nguyen, Prema, Buza, and Dzigal models. Our benchmark for validating our combination proposal is a comparison using the outputs calculated by the complete rule assembled of the fire detection algorithms.

Since our proposal combines knowledge of fire detection at the gray level, we require a quantitative threshold stage to assess binary segmentation. For this purpose, we used the widely accepted binarization method of Otsu [68]. This method allowed us to compare the outcome of our proposal with the ground truth of the dataset. Furthermore, we compare our combination method to two frequently used techniques for the combination of binary labels [69], [70], [71]: majority voting and the weighted majority voting scheme. The simple majority was used in the majority voting scheme. However, the weights assigned in the weighted majority voting scheme were assigned using the IoU metric computed from our test series.

To statistically validate the results of our combination approach, we performed 30 experiments. To carry out our experiments, we split the dataset: training images subset 50%, selection images subset 10%, and test images subset 40%. The training partition of the dataset is utilized to evolve the individuals in the population. Subsequently, we selected the best individual from each experiment, resulting in 30 individuals, our combination rule-based models. The best 30 individuals are tested using the selection partition subset. We perform bootstrap to calculate the median and confidence intervals (CI) at 95% to select the best model computed from the experiments. The individual computing with the best performance is selected as the top model obtained from the 30 experiments carried out. We utilized the MCC metric to evaluate the models in this stage. Finally, we assess the performance of our proposal and the other methods using the test image subset. We used the F-measure and the IoU metrics at this stage to evaluate.

D. PARAMETERS SETTING OF THE EVOLUTIONARY PROPOSAL

The proposed evolutionary approach requires the setting of critical parameters to ensure the correct evolution of the individuals. As we mentioned earlier, the structure utilized to encode the combination model was the tree structure. We specified the initial length of the individuals to 5. However, it was allowed to grow to 10 during evolution. In our experiments, we determined that setting the initial population at 100 individuals adequately obtains a reliable model. In addition, we set the number of generations to 30.

The mating set is retrieved from the population using the roulette wheel selection method. The probability of selection of individuals is proportionally determined by the score obtained for the fitness function utilized. We resolved to select 20 individuals to create ten couples, and we set the offspring at 20. The one-point crossover is performed on the tree's nodes, where the node can be a terminal or a function. The crossover is carried out by replacing the entire branch downward from the selected node.

To validate the individuals, we proposed to utilize the Matthews Correlation Coefficient (MCC) metric as our fitness function J. The MCC metric yields are more informative and reliable in measuring binary classification tasks [72], [73]. In Equation 40, we define the MCC metric,

$$MCC = \frac{(TP \times TN) - (FP \times FN)}{(TP+FP)\times(TP+FN)\times(TN+FP)\times(TN+FN)}. \tag{40}$$

The validation of the individuals is performed by assessing the binary fire-pixel segmentation. Our proposal combines fire detection rules so that the output obtained is given at a gray level. Therefore, we require a binarization stage to validate each individual as a plausible combination model. In our proposal, we used the Otsu thresholding algorithm [68]. The following population is selected by retaining the best 90% of the population; in this manner, we implement the elitist strategy by preserving the best individual. In addition, we set an individual's mutation probability at 5%. Table 7 presents a summary of the parameters used to evolve the model for our experiments and the effect on the results obtained.

The following paragraphs present an analysis of the complexity of the proposed evolutionary approach. The experiments were carried out on computational equipment configured with Intel(R) Core(TM) i7-11800H @ 2.30GHz and 32 GB of RAM memory. The complexity analysis was performed by varying the parameter of the size of the initial population while we fixed the rest of the parameters. Some authors claim that various parameters influence the complexity of evolutionary approaches [74]. The size of the population is considered one of the most critical parameters that affects the complexity of the algorithm [75].

To analyze the complexity of our approach, we vary the size of the initial population to 50, 100, and 150 individuals. Table 8 summarizes the convergence time for each initial population size. Furthermore, we evaluated the best model obtained from each experiment in the validation dataset using the MCC metric. From the table, we observe that the size of the initial population influences the convergence time of our approach: larger initial populations result in longer convergence times. However, evaluating the models on the validation data set does not show significant differences.

TABLE 7. Summary of the parameters utilized for the proposed approach.

Parameter	Value	Result	Critical remark
Initial population	100	Improved diversity	The larger the size, the larger the computational time
Number of offspring	20	Improvements to existing solutions	Maintaining trade-off between exploration of the search space and computational cost
Number of generations	30	Converges towards optimal solutions	Increasing generations resulted in no significant better results
Mating set size	20	Emphasized exploitation of the best individuals	Mating set size have a direct influence on genetic diversity
Mutation probability	5%	Exploring the less-explored areas of the search space	High mutation rate eliminates the evolutionary advantage
Fitness function	MCC metric	Allows the assessment of the solutions	To assess the individuals using the proposed fitness function, we include a binarization stage
Mating set selection	Roulette wheel	The best individuals were selected to improve the solution	Biased toward fitter individuals
Selection strategy	Elitism strategy	Preserves the best solutions	Excessive elitism reduces diversity and exploration

TABLE 8. Summary of the convergence time for each initial population analyzed and average performance on the validation dataset.

Initial population	Convergence time (s)	MCC on the validation data
50	7532	0.918
100	8584	0.908
150	10006	0.913

In Figure 5, we show the memory usage throughout the model evolution. From the figure, it can be observed that the memory consumption of our approach tends to increase with the size of the initial population and continues to grow as the offspring stage progressively increases the number of individuals during the evolution.

In addition, we present the calculation cost of the proposed method. In Table 9, the average time taken to calculate the fire segmentation on the validation image subset is presented. In addition, the average memory usage during the fire segmentation on the validation image subset is included. In our proposal, the fire pixel segmentation was performed in an average time of 0.019 seconds, while the average memory used to compute fire pixel segmentation was 1.19 MB. It is worth mentioning that the features used for combining were calculated previously.

TABLE 9. Calculation cost of the proposed approach. The time and memory were calculated by averaging in the validation image subset.

Average time (s)	Average memory usage (MB)
0.019	1.19

E. ANALYSIS OF THE RULE-BASED COMBINATION MODEL

The parameters defined previously determine the evolution of the aggregation model. Figure 6 presents an example of the average performance over the 30 generations. From the figure, we can observe that the overall performance of the population improves over generations. In addition, the standard deviation performance of individuals tends to decrease. In the final generations, small increments of improvement in individuals' average performance indicate that the system is converging toward an optimal solution. In Figure 7, we show the validation of our experiments. We perform bootstrap to validate the model's performance obtained from the 30 experiments. From the figure, we can observe that the 30 models computed present a similar behavior. Since the CI of the models overlaps, we select the model that scores higher in mean value.

In figure 8, we give an example of an individual obtained from our evolutionary proposal. The combination is performed from the bottom level of the tree structure up to the top level. The individual comprises fuzzy operators that perform operations on the maps computed from the modified rules. For each function, we compute a fusion of two features. The last level of the individual is always composed of terminals. On the contrary, the root of the tree structure is always a function.

The proposed system explores plausible combination models. We analyze the frequency of use of terminals and functions by our system during the search for the optimal combination model. In Table 10, we present a descriptive analysis of the frequency of rule use when building the combination model. The r_1 rule was the most used, 7.40%, when searching for the optimal model. The r_{12} was used 7.17% and the r_{17} rule was used 6.39%. The analysis of the usage of the functions is given in Table 11. The minimum was the most used fuzzy operator, 13.67%. The bounded difference of the operator was used in 13.21%, and the product operator was used in 12.18%.

The proposed system aims to identify the optimal model for aggregating fire detection knowledge by utilizing various fire models and fuzzy operators. In Table 12, we computed the occurrence of the terminals and operators in the best

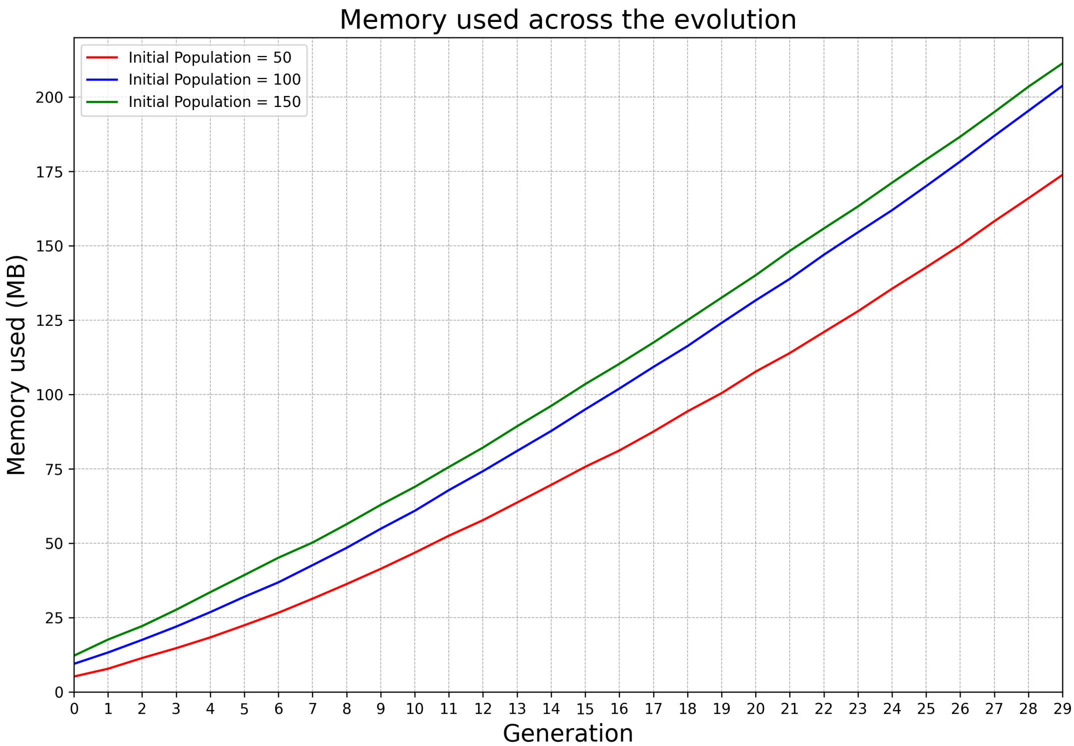

FIGURE 5. Memory usage across the evolution of the different sizes of the initial population.

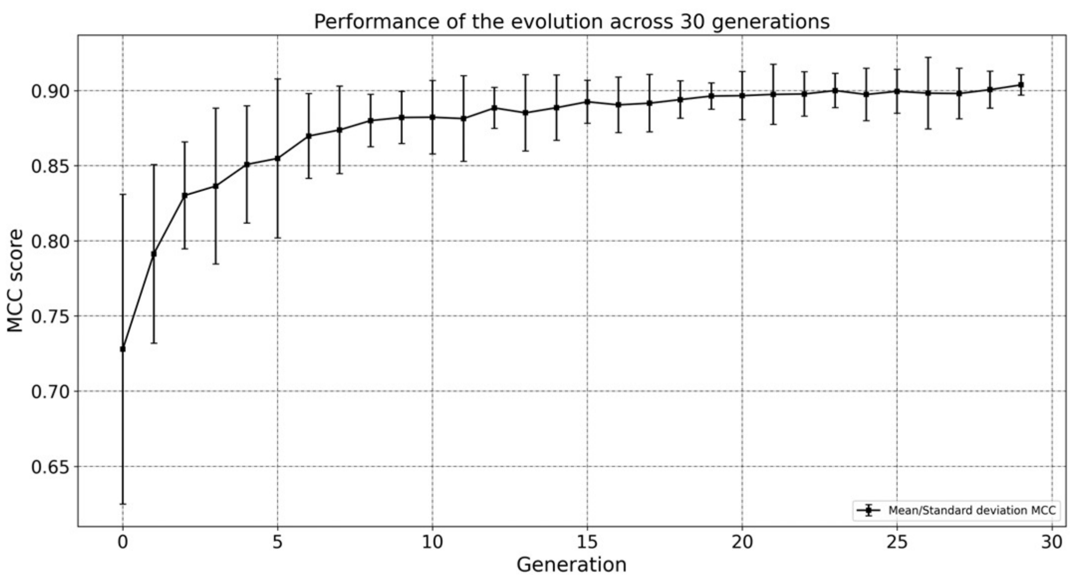

FIGURE 6. Sample of the evolution of one of the experiments performed. The MCC average performance and standard deviation are given.

individual of each experiment. Essentially, we analyze the composition of the top 30 individuals generated from our experiments. The r_1 rule was used at 12.66%. The r_9 rule was utilized at 12.03%. In contrast, the rule r_{23}% was excluded from the final solution found in the proposal. In Table 13, we summarize the most commonly used fuzzy operators that

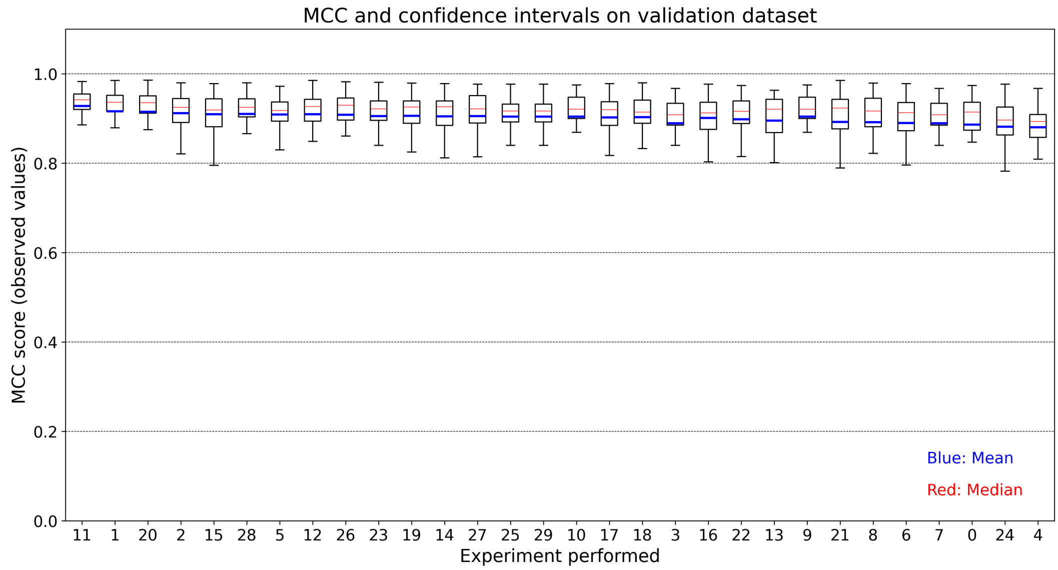

FIGURE 7. Example of the validation of the best models for each experiment.The experiments are ordered from best to worst (left to right).The C.I. is calculated by performing bootstrap. In blue, the mean value is computed. In red, the median value is calculated.

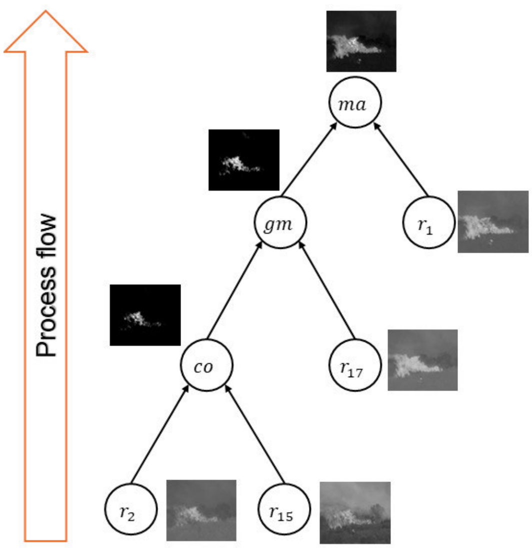

FIGURE 8. Example of combination model obtained from our proposal. The model comprises fuzzy operators and feature maps computed from the rules.

make up the best combination models. The most widely used function is the symmetric sum at 14.84%. The product and the bounded difference were used at 11.72% in the best individuals. In contrast to the terminals, all fuzzy operators were used in the final combination models.

IV. RESULTS

In this section, we present the results obtained from our test series described in Section III-C. We present qualitative and quantitative results. First, we qualitatively compare the output image obtained by our approach to the results obtained by state-of-the-art fire detection methods. Secondly,

TABLE 10. Analysis of the importance of the terminals utilized by our combination approach. We count the frequency of usage for fire detection rules during the system's evolving process as part of the model development.

Terminal	Author	Percent used
$r_1 = R - G$	Nguyen	7.40 %
$r_2 = G - B$	Nguyen	4.39 %
$r_3 = R - R_{th}$	Nguyen	5.78 %
$r_4 = G - G_{th}$	Nguyen	1.51 %
$r_5 = B_{th} - B$	Nguyen	1.41 %
$r_6 = Y - C_r$	Nguyen	1.04 %
$r_7 = C_r - C_b$	Nguyen	5.39 %
$r_8 = Y - \mu_Y$	Nguyen	2.40 %
$r_9 = C_r - \mu_{C_r}$	Nguyen	5.94 %
$r_{10} = \mu_{C_b} - C_b$	Nguyen	6.17 %
$r_{11} = Y - C_b$	Prema	1.85 %
$r_{12} = C_r - C_b$	Prema	7.17 %
$r_{13} = \lvert C_b - C_b) \rvert - T$	Prema	6.28 %
$r_{14} = I'_{[R]} - \mu_R$	Buza	1.48 %
$r_{15} = I'_{[G]} - \mu_G$	Buza	1.87 %
$r_{16} = I'_{[B]} - \mu_B$	Buza	2.66 %
$r_{17} = I'_{[R]} - I'_{[B]}$	Buza	6.39 %
$r_{18} = (I'_{[R]} + I'_{[B]}) - I'_{[G]}$	Buza	2.79 %
$r_{19} = S - 35$	Dizigal	3.55 %
$r_{20} = 65 - H$	Dizigal	3.80 %
$r_{21} = H - 330$	Dizigal	1.80 %
$r_{22} = L - 70$	Dizigal	1.78 %
$r_{23} = \mu_B - B$	Dizigal	4.13 %
$r_{24} = \mu_W - W$	Dizigal	2.22 %
$r_{25} = W - \mu_W$	Dizigal	1.92 %
$r_{26} = S - \mu_S$	Dizigal	3.51 %
$r_{27} = W - 98$	Dizigal	1.98 %
$r_{28} = 2 - B$	Dizigal	3.40 %

TABLE 11. Analysis of the importance of the functions utilized by our combination approach. We count the times our system utilized each fuzzy operator.

Terminal	Type	Percent used
$min\{A, B\}$	Minimum	13.67 %
AB	Product	12.18 %
$max\{0, A+B-1\}$	Bounded difference	13.21 %
$max\{A, B\}$	Maximum	9.01 %
$A+B-AB$	Probabilistic sum	4.25 %
$min\{1, A+B\}$	Bounded sum	3.78 %
$min\{1, 1-A+B\}$	Lukasiewicz	3.26 %
$max\{1-A, B\}$	Klen-Dienes	1.95 %
$\sqrt{AB}$	Geometric mean	8.54 %
$\frac{2AB}{A+B}$	Harmonic mean	11.21 %
$\frac{A+B-AB}{1+A+B-2AB}$	Symmetric sum	6.74%
$\frac{AB}{1-A-B+2AB}$	Symmetric sum	12.17 %

TABLE 12. Analysis of the top 30 models. The best model from each experiment is analyzed. Terminal usage is represented as a percentage. We examine the composition of the best individual from each experiment conducted.

Terminal	Author	Percent used
$r_1 = R - G$	Nguyen	12.66 %
$r_2 = G - B$	Nguyen	1.27 %
$r_3 = R - R_{th}$	Nguyen	1.27 %
$r_4 = G - G_{th}$	Nguyen	1.27 %
$r_5 = B_{th} - B$	Nguyen	1.27 %
$r_6 = Y - C_r$	Nguyen	1.27 %
$r_7 = C_r - C_b$	Nguyen	6.33 %
$r_8 = Y - \mu_Y$	Nguyen	0.63 %
$r_9 = C_r - \mu_{C_r}$	Nguyen	12.03 %
$r_{10} = \mu_{C_b} - C_b$	Nguyen	2.53 %
$r_{11} = Y - C_b$	Prema	0.63 %
$r_{12} = C_r - C_b$	Prema	10.13 %
$r_{13} = \lvert C_b - C_b) \rvert - T$	Prema	11.39 %
$r_{14} = I'_{[R]} - \mu_R$	Buza	5.70 %
$r_{15} = I'_{[G]} - \mu_G$	Buza	0.63 %
$r_{16} = I'_{[B]} - \mu_B$	Buza	2.53 %
$r_{17} = I'_{[R]} - I'_{[B]}$	Buza	3.16 %
$r_{18} = (I'_{[R]} + I'_{[B]}) - I'_{[G]}$	Buza	3.80 %
$r_{19} = S - 35$	Dizigal	0.63 %
$r_{20} = 65 - H$	Dizigal	4.43 %
$r_{21} = H - 330$	Dizigal	0.0 %
$r_{22} = L - 70$	Dizigal	2.53 %
$r_{23} = \mu_B - B$	Dizigal	3.80 %
$r_{24} = \mu_W - W$	Dizigal	2.53 %
$r_{25} = W - \mu_W$	Dizigal	1.27 %
$r_{26} = S - \mu_S$	Dizigal	3.8 %
$r_{27} = W - 98$	Dizigal	1.27 %
$r_{28} = 2 - B$	Dizigal	1.27 %

TABLE 13. Analysis of the top 30 models. The best model from each experiment is analyzed. Functions usage is represented as a percentage. We examine the composition of the best individual from each experiment conducted.

Terminal	Type	Percent used
$min\{A, B\}$	Minimum	8.59 %
AB	Product	11.72 %
$max\{0, A+B-1\}$	Bounded difference	11.72 %
$max\{A, B\}$	Maximum	6.25 %
$A+B-AB$	Probabilistic sum	6.25 %
$min\{1, A+B\}$	Bounded sum	7.03 %
$min\{1, 1-A+B\}$	Lukasiewicz	4.69 %
$max\{1-A, B\}$	Klen-Dienes	2.34 %
$\sqrt{AB}$	Geometric mean	10.16 %
$\frac{2AB}{A+B}$	Harmonic mean	9.38 %
$\frac{A+B-AB}{1+A+B-2AB}$	Symmetric sum	14.84 %
$\frac{AB}{1-A-B+2AB}$	Symmetric sum	7.03 %

we quantitatively evaluated the performance of our proposal and the state-of-the-art methods using two widely used binary classification assessment metrics. The quantitative result is threefold. We assess our proposal and the state-of-the-art techniques at the individual rule-wise level. Second, we evaluate the results obtained from our proposal and the rest of the approaches at the method-wise level; that is, we utilize the complete implementation of color-based fire models.

Finally, we compare our results with the aggregation approach proposed in [34] and with two well-accepted binary label combination techniques, majority voting, and the weighted majority voting approach. All experiments were performed using the F-score metric and the IoU metric.

A. QUALITATIVE COMPARISON

We performed a qualitative comparison of the outcomes calculated by our proposal and the state-of-the-art methods. Firstly, we present a qualitative comparison of the outcomes computed using the individual rules and our method. Secondly, we compare the results obtained from the fire detection methods with our proposal.

In Figure 9, we present the results computed from the individual rules. From that figure, we can observe that the fire maps calculated by the individual rules exhibit outputs that fail by over-segmenting the fire scene. In contrast, the outputs obtained from our combination approach are similar to the ground truth without any postprocessing stage. Individual rules' failures may arise from their role within a rule-based composite fire detection model, in which the authors use a subset of individual rules to perform fire detection in conjunction. On the other hand, in Figure 10, we compare

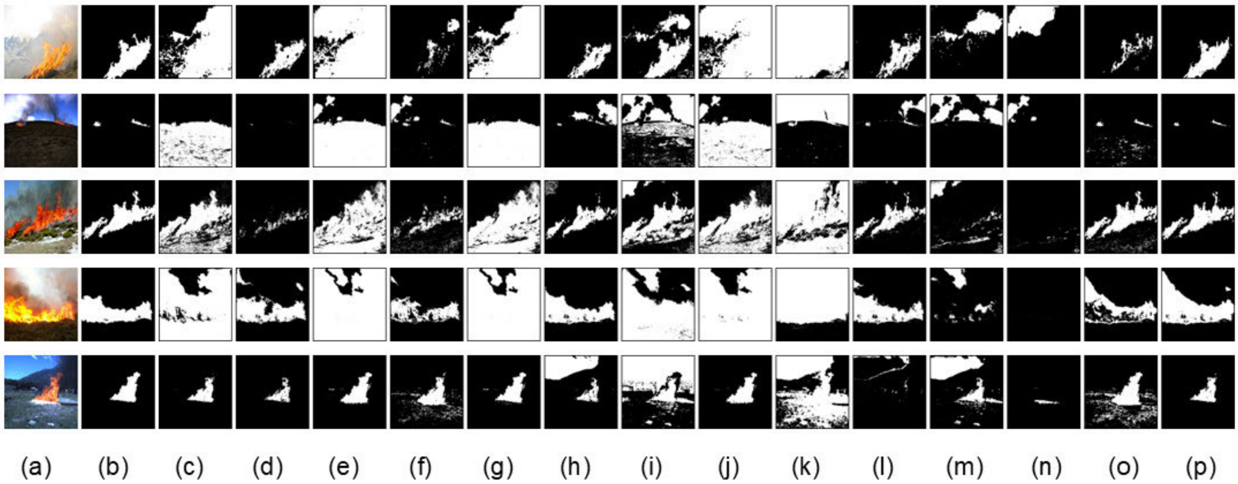

FIGURE 9. Comparison of the results obtained from the individual rules. (a) Input image. (b) Ground truth. (c) $Rule_1$ (Nguyen). (d) $Rule_2$ (Nguyen). (e) $Rule_3$ (Nguyen). (f) $Rule_4$ (Nguyen). (g) $Rule_5$ (Prema). (h) $Rule_6$ (Prema). (i) $Rule_7$ (Buza). (j) $Rule_8$ (Dzigal). (k) $Rule_9$ (Dzigal). (l) $Rule_{10}$ (Dzigal). (m) $Rule_{11}$ (Dzigal). (n) $Rule_{12}$ (Dzigal). (o) $Rule_{13}$ (Dzigal). (p) Our method.

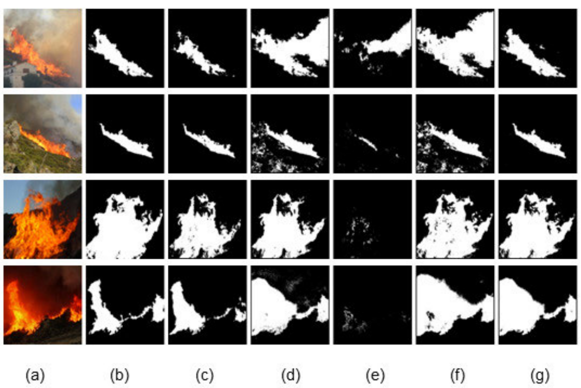

FIGURE 10. Qualitative comparison of the results obtained from other fire detection methods and our approach. (a) Input image. (b) Ground truth. (c) Prema. (d) Dzigal. (e) Nguyen. (f) Buza. (p) Our method.

the outputs obtained from the fire detection methods and our proposal. That figure shows that the results obtained from the complete rule-based color model tend to be better than those from individual rules. Nevertheless, the outputs obtained from our proposal are similar to the ground truth in most of the examples presented.

B. EVALUATION OF FIRE DETECTION INDIVIDUAL RULES AND OUR PROPOSAL

We conducted an experiment based on individual rules to validate that our proposed method improves fire detection. That is, we utilize each rule, comprising the fire detection approaches, to compute fire detection. Hence, we compare our proposal with 13 different rules for fire detection.

In Table 14, we present the comparison of the rules as individual entities and our proposal. From Table 14, we can observe that $Rule_2$ of the Nguyen model achieved the best precision score of 0.923. On the other hand, our proposal scored 0.823, and $Rule_6$ of the Prema model obtained 0.895. The worst precision performance was obtained by $Rule_{13}$ of the Dzigal model, which scored 0.114. Regarding the recall metric, the best score is obtained by $Rule_5$ of the Prema method that achieved 0.993. The $Rule_9$ of the Dzigal method scored 0.986, and $Rule_3$ of the Nguyen model obtained 0.988. In contrast, our proposed method achieved a score of 0.881. The $Rule_{13}$ of the Dizgal model presented a poor performance, which scored 0.002. Our proposal achieves the highest F-score metric, which scored 0.815. In contrast, $Rule_7$ of the Buza method obtained a score of 0.714, and $Rule_4$ of the Nguyen model calculated 0.664.

TABLE 14. Comparison using F-measure. Each rule is evaluated individually yo our proposal.

Rule	Precision	Recall	F-measure
$Rule_1$ $(Nguyen)$	0.409	0.930	0.526
$Rule_2$ $(Nguyen)$	**0.923**	0.528	0.635
$Rule_3$ $(Nguyen)$	0.315	0.987	0.443
$Rule_4$ $(Nguyen)$	0.722	0.701	0.664
$Rule_5$ $(Prema)$	0.319	**0.993**	0.449
$Rule_6$ $(Prema)$	0.895	0.560	0.647
$Rule_7$ $(Buza)$	0.661	0.898	0.714
$Rule_8$ $(Dzigal)$	0.528	0.868	0.603
$Rule_9$ $(Dzigal)$	0.352	0.988	0.485
$Rule_{10}$ $(Dzigal)$	0.296	0.956	0.411
$Rule_{11}$ $(Dzigal)$	0.761	0.560	0.606
$Rule_{12}$ $(Dzigal)$	0.485	0.278	0.291
$Rule_{13}$ $(Dzigal)$	0.114	0.002	0.004
Our method	0.823	0.881	**0.815**

Given the results presented in Table 14, we can observe that our proposal obtained a more balanced performance in precision and recall metrics, causing a higher F-measure with respect to the rest of the state-of-the-art rules. Despite our proposal being overcome in terms of precision and recall, the state-of-the-art rules tend to be unbalanced, causing underperformance.

TABLE 15. Comparison using IoU metric. Each rule is evaluated individually against our proposal.

Rule	IoU
$Rule_1$ $(Nguyen)$	0.386
$Rule_2$ $(Nguyen)$	0.497
$Rule_3$ $(Nguyen)$	0.311
$Rule_4$ $(Nguyen)$	0.535
$Rule_5$ $(Prema)$	0.317
$Rule_6$ $(Prema)$	0.519
$Rule_7$ $(Buza)$	0.596
$Rule_8$ $(Dzigal)$	0.473
$Rule_9$ $(Dzigal)$	0.348
$Rule_{10}$ $(Dzigal)$	0.285
$Rule_{11}$ $(Dzigal)$	0.473
$Rule_{12}$ $(Dzigal)$	0.196
$Rule_{13}$ $(Dzigal)$	0.002
Our method	**0.728**

TABLE 16. Comparison, using F-measure, of the fully implemented color-based fire detection models and our approach.

Rule	Precision	Recall	F-measure
Prema (2018)	**0.950**	0.446	0.570
Dzigal (2019)	0.846	0.793	0.787
Buza (2022)	0.661	**0.898**	0.714
Nguyen (2022)	0.847	0.155	0.240
Our method	0.823	0.881	**0.815**

In addition, in our test series, we assess our proposal and the rules of the top methods using the IoU metric. From Table 15, we can observe that our proposal obtained the best performance of 0.728. In contrast, the $Rule_7$ of the Buza method obtained 0.596, and the $Rule_6$ of the Prema method scored 0.519. Our proposal outperforms the rest of the state-of-the-art rules regarding the IoU metric, indicating that it overcomes the classification of non-fire and fire pixels.

C. EVALUATION OF FIRE DETECTION METHODS AND OUR PROPOSAL

In this section, we present the results obtained from our series of tests using the outputs of four state-of-the-art models and our approach. Specifically, we performed experiments using the complete implementation of Prema, Dzigal, Buza, and Nguyen fire detection models.

From Table 16, we can observe that the Prema model obtained the best precision score of 0.955. However, our proposal achieved a precision score of 0.881, and the Dzigal model scored 0.841. The Buza model achieved the best performance of 0.890 with respect to the recall metric. In contrast, our approach scored a recall of 0.837, while the Dzigal model achieved a score of 0.787. Our proposed method obtained the best F-score of 0.838. In contrast, Dzigal scored 0.779, and the Buza and Nguyen models attained 0.697.

Even though the proposed method attained lower precision and recall metrics than the Prema and Buza models, respectively, our proposal obtained a competitive and balanced precision and recall and, consequently, attained the best performance in terms of the F score.

TABLE 17. Comparison, using IoU, of the fully implemented color-based fire detection models and our approach.

Rule	IoU
Prema (2018)	0.436
Dzigal (2019)	0.676
Buza (2022)	0.596
Nguyen (2022)	0.150
Our method	**0.728**

Table 17 compares the results using the IoU metric. Our method obtained a higher IoU score of 0.736. The model proposed by Dizgal obtained an IuO score of 0.665. In contrast, the Buza model scored 0.580. According to the computed results, the proposed model achieved the highest IoU score, surpassing the results obtained from the fire detection models used for comparison.

In summary, our proposed combination system achieved better results than the individual rules and models of various authors. According to the results presented previously, the combination of rules assists in obtaining enhanced fire detection models.

D. COMBINATION METHODS COMPARISON

Additionally, we compare the performance of our approach with the approach proposed by Buza et al. in [34] and two widely accepted binary label combination approaches. We precisely assess performance using the *"and"* operator to combine the best rules, the majority voting technique, and the weighted majority voting approach. In order to perform the combination proposed in [34], we rank the individual rules using the F-measure calculated in the previous experiment presented in Table 14. In our experiments, we used the top six individual rules to implement the Buza approach.

First, we compare the results of combining individual rules using majority voting, weighted majority voting, and our approach. In Table 18, we present the results obtained from our experiments. The Top 1 & Top 3 combination scores 0.957. The weighted majority vote reached 0.927 similar to the Top 1 & Top 4 pair combination. The proposed method achieved a precision score of 0.8.23. The best recall score was obtained using the majority vote technique, which scored 0.892. In contrast, our proposal achieved 0.881 and the Top 1 & Top 5 combination scored 0.801. The proposed fuzzy aggregation achieved 0.815 in the F-measure. In contrast, the Top 1 & Top 5 combination achieved 0.777, while weighted majority voting obtained 0.630.

Regarding the IoU metric, our proposal obtained the best score of 0.728. In contrast, the Top 1 & Top 5 scored 0.664 and the Top 1 & Top 4 achieved 0.532. Our proposal consistently overcomes other fusion approaches in the F-measure and the IoU metric. Despite the majority vote technique overcoming our proposal in recall metrics, our approach achieved competitive performance.

Second, we assess the combination of methods using the strategy proposed by Buza, the majority vote technique, and the weighted majority voting. From Table 19, we can observe

TABLE 18. Assessment, in terms of F-score and IoU metric, of the combination of individual rules using majority voting, weighted majority voting, and our approach.

Combination technique	Precision	Recall	F-measure	IoU
Majority voting	0.551	**0.892**	0.591	0.465
Weighted majority voting	0.927	0.520	0.630	0.491
Top 1 & Top 2 [34]	0.742	0.684	0.661	0.531
Top 1 & Top 3 [34]	**0.957**	0.531	0.642	0.513
Top 1 & Top 4 [34]	0.927	0.502	0.621	0.532
Top 1 & Top 5 [34]	0.823	0.801	0.777	0.664
Top 1 & Top 6 [34]	0.846	0.551	0.620	0.485
Our method	0.823	0.881	**0.815**	**0.728**

TABLE 19. Assessment, in terms of F-score and IoU metric, of the combination of the complete methods using majority voting, weighted majority voting, and our approach.

Combination technique	Precision	Recall	F-measure	IoU
Majority voting	0.757	0.866	0.762	0.651
Weighted majority voting	**0.966**	0.448	0.576	0.440
Top 1 & Top 2 [34]	0.855	0.767	0.776	0.660
Top 1 & Top 3 [34]	0.953	0.441	0.561	0.433
Top 1 & Top 3 [34]	0.899	0.145	0.231	0.661
Our method	0.823	**0.881**	**0.815**	**0.728**

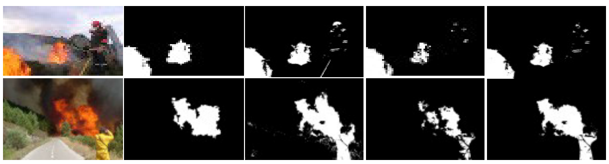

(a) (b) (c) (d) (e)

FIGURE 11. Samples of failure cases. Our proposal misclassifies color-fire objects. (a) Input image. (b) Ground truth. (c) Prema. (d) Dzigal. (e) Our method.

that our proposal was calculated in precision as 0.823, while the weighted majority voting scored 0.966, and the Top 1 & Top 3 was calculated as 0.953. Our approach obtained the best recall of 0.881. In contrast, the majority approach achieved 0.866, and the Top 1 & Top 2 obtained 0.767. Our proposal obtained an F-measure of 0.815. The majority vote scored 0.762, and the Top 1 & Top 2 obtained 0.776.

Similarly, our proposal overcomes the fusion approaches in terms of the IoU metric, scoring 0.728. The pair of methods Top 1 & Top 3 scored 0.661, and the Top 1 & Top 2 calculated 0.660. According to the previous results, our proposal performed the best compared to other combination approaches at the individual rule and method levels.

Although the proposal improves fire pixel segmentation, our method does not effectively distinguish fire-colored objects, leading to misclassification of pixels. In Figure 11, we present some samples of images containing distractors. We can observe that our proposal fails similarly to the other methods that misclassify fire-color objects as fire pixels. It is worth mentioning that a different feature of color is needed to overcome the limitations of using just color information.

The presented results show that our proposal retrieves a competitive number of fire pixels without significant loss in precision. Precision is a metric for assessing the accuracy of the model in classifying the target class, while the recall metric assesses the capability of the model to identify all relevant instances. Contrary to the rule-based models discussed above, the proposed method realizes a balanced trade-off between precision and recall, improving overall performance.

V. CONCLUSION

In this research work, we present a system that combines various fire-pixel segmentation rules. The proposed method modifies inequality-based rules into a subtraction operation to compute a fire map at the gray level. The proposed approach utilizes fuzzy operators to combine the outcomes of various rules. Additionally, a genetic algorithm is employed to fine-tune the rule-based combination model. The combination model is encoded in a tree structure, with nodes that can be terminals or functions, leaves that represent terminals, and a root that represents a function.

The proposed model has been evaluated on the challenging and widely used CORSICAN dataset, which was explicitly designed to evaluate fire segmentation models. Our proposal's results were compared with four state-of-the-art fire color models: Prema, Dzigal, Buza, and Nguyen. Additionally, we evaluate the performance of our approach alongside two binary label combination strategies: the expert system technique using majority voting and the weighted majority voting technique. The results of the test series indicate that our method outperforms the four individual methods in the two quantitative metrics used to evaluate our proposal. Despite our method achieving a higher F-measure, the precision and recall metrics ranked second. However, our method's precision, recall, and F-measure are more balanced than those of the other methods. In addition, the proposed method achieves better performance when assessed using the IoU metric. The majority vote techniques were used to evaluate the performance of our model. Our method achieved a higher F-measure and precision, while the recall metric ranked second. Similarly, our proposed method demonstrates better performance in the IoU metric.

The rule most commonly used in the models of each experiment was r_1 of the Nguyen method. The background content of the forest probably supports the use of the r_1 rule, which is expressed as the difference between the R and G channels. The symmetric sum was the fuzzy operator that was used the most frequently in the top models of the experiments. The use of the symmetric sum in the final combination model suggests that our approach successfully combines the methods by searching for intermediate values to compensate for the constraints of using only the maximum and minimum operators.

Our method improves fire-pixel segmentation by combining knowledge from various color-based fire-pixel segmentation models. The resulting combination model is simple and remains human-comprehensible. However, the performance of our method is limited by the knowledge available from the combined fire models. Therefore, in future research, we aim to develop a system that designs its features, overcoming the limitations of color-based features by incorporating additional characteristics such as texture, movement, and others.

REFERENCES

[1] S. Li and T. Banerjee, "Spatial and temporal pattern of wildfires in California from 2000 to 2019," *Sci. Rep.*, vol. 11, no. 1, p. 8779, Apr. 2021.

[2] J. G. Pausas and J. E. Keeley, "Wildfires and global change," *Frontiers Ecol. Environ.*, vol. 19, no. 7, pp. 387–395, Jun. 2021.

[3] A. Bouguettaya, H. Zarzour, A. M. Taberkit, and A. Kechida, "A review on early wildfire detection from unmanned aerial vehicles using deep learning-based computer vision algorithms," *Signal Process.*, vol. 190, Jan. 2022, Art. no. 108309.

[4] I. El-Madafri, M. Peña, and N. Olmedo-Torre, "Dual-dataset deep learning for improved forest fire detection: A novel hierarchical domain-adaptive learning approach," *Mathematics*, vol. 12, no. 4, p. 534, Feb. 2024.

[5] H. Harkat, J. M. P. Nascimento, A. Bernardino, and H. F. T. Ahmed, "Fire images classification based on a handcraft approach," *Expert Syst. Appl.*, vol. 212, Feb. 2023, Art. no. 118594.

[6] A. Gaur, A. Singh, A. Kumar, A. Kumar, and K. Kapoor, "Video flame and smoke based fire detection algorithms: A literature review," *Fire Technol.*, vol. 56, no. 5, pp. 1943–1980, Sep. 2020.

[7] E. Buza and A. Akagic, "Unsupervised method for wildfire flame segmentation and detection," *IEEE Access*, vol. 10, pp. 55213–55225, 2022.

[8] T. Celik, H. Demirel, H. Ozkaramanli, and M. Uyguroglu, "Fire detection using statistical color model in video sequences," *J. Vis. Commun. Image Represent.*, vol. 18, no. 2, pp. 176–185, Apr. 2007.

[9] P.-H. Huang, J.-Y. Su, Z.-M. Lu, and J.-S. Pan, "A fire-alarming method based on video processing," in *Proc. Int. Conf. Intell. Inf. Hiding Multimedia*, Dec. 2006, pp. 359–364.

[10] B. U. Töreyin, Y. Dedeoğlu, U. Güdükbay, and A. E. Çetin, "Computer vision based method for real-time fire and flame detection," *Pattern Recognit. Lett.*, vol. 27, no. 1, pp. 49–58, Jan. 2006.

[11] V. Vipin, "Image processing based forest fire detection," *Int. J. Emerg. Technol. Adv. Eng.*, vol. 2, no. 2, pp. 87–95, 2012.

[12] W. Phillips III, M. Shah, and N. da Vitoria Lobo, "Flame recognition in video," *Pattern Recognit. Lett.*, vol. 23, nos. 1–3, pp. 319–327, Jan. 2002.

[13] D. Y. T. Chino, L. P. S. Avalhais, J. F. Rodrigues, and A. J. M. Traina, "BoWFire: Detection of fire in still images by integrating pixel color and texture analysis," in *Proc. 28th SIBGRAPI Conf. Graph., Patterns Images*, Aug. 2015, pp. 95–102.

[14] Jubeena. B. Maheen and R. P. Aneesh, "Machine learning algorithm for fire detection using color correlogram," in *Proc. 2nd Int. Conf. Intell. Comput., Instrum. Control Technol. (ICICICT)*, vol. 1, Jul. 2019, pp. 1411–1418.

[15] A. Krizhevsky, I. Sutskever, and G. E. Hinton, "ImageNet classification with deep convolutional neural networks," *Commun. ACM*, vol. 60, no. 6, pp. 84–90, May 2017.

[16] S. Frizzi, R. Kaabi, M. Bouchouicha, J.-M. Ginoux, E. Moreau, and F. Fnaiech, "Convolutional neural network for video fire and smoke detection," in *Proc. 42nd Annu. Conf. IEEE Ind. Electron. Soc.*, Oct. 2016, pp. 877–882.

[17] Y. Zhao, J. Ma, X. Li, and J. Zhang, "Saliency detection and deep learning-based wildfire identification in UAV imagery," *Sensors*, vol. 18, no. 3, p. 712, Feb. 2018.

[18] A. Jadon, M. Omama, A. Varshney, M. S. Ansari, and R. Sharma, "FireNet: A specialized lightweight fire & smoke detection model for real-time IoT applications," 2019, *arXiv:1905.11922*.

[19] A. Shees, M. S. Ansari, A. Varshney, M. N. Asghar, and N. Kanwal, "FireNet-v2: Improved lightweight fire detection model for real-time IoT applications," *Proc. Comput. Sci.*, vol. 218, pp. 2233–2242, Jan. 2023.

[20] K. Napierala and J. Stefanowski, "BRACID: A comprehensive approach to learning rules from imbalanced data," *J. Intell. Inf. Syst.*, vol. 39, no. 2, pp. 335–373, Oct. 2012.

[21] M. Setnes, R. Babuska, and H. B. Verbruggen, "Rule-based modeling: Precision and transparency," *IEEE Trans. Syst., Man Cybern., C, Appl. Rev.*, vol. 28, no. 1, pp. 165–169, Jan. 1998.

[22] C. Lang, G. Cheng, B. Tu, and J. Han, "Few-shot segmentation via divide-and-conquer proxies," *Int. J. Comput. Vis.*, vol. 132, no. 1, pp. 261–283, Jan. 2024.

[23] C. Lang, G. Cheng, B. Tu, and J. Han, "Learning what not to segment: A new perspective on few-shot segmentation," in *Proc. IEEE/CVF Conf. Comput. Vis. Pattern Recognit. (CVPR)*, Jun. 2022, pp. 8047–8057.

[24] C. Lang, G. Cheng, B. Tu, C. Li, and J. Han, "Base and meta: A new perspective on few-shot segmentation," *IEEE Trans. Pattern Anal. Mach. Intell.*, vol. 45, no. 9, pp. 10669–10686, Sep. 2023.

[25] G. Cheng, C. Lang, and J. Han, "Holistic prototype activation for few-shot segmentation," *IEEE Trans. Pattern Anal. Mach. Intell.*, vol. 45, no. 4, pp. 4650–4666, Apr. 2023.

[26] X. Liu, L. Song, S. Liu, and Y. Zhang, "A review of deep-learning-based medical image segmentation methods," *Sustainability*, vol. 13, no. 3, p. 1224, Jan. 2021.

[27] S. Minaee, Y. Boykov, F. Porikli, A. Plaza, N. Kehtarnavaz, and D. Terzopoulos, "Image segmentation using deep learning: A survey," *IEEE Trans. Pattern Anal. Mach. Intell.*, vol. 44, no. 7, pp. 3523–3542, Jul. 2022.

[28] Z. Chen, H. Zhou, J. Lai, L. Yang, and X. Xie, "Contour-aware loss: Boundary-aware learning for salient object segmentation," *IEEE Trans. Image Process.*, vol. 30, pp. 431–443, 2021.

[29] M. Detyniecki, "Fundamentals on aggregation operators," Comput. Sci. Division, Univ. California at Berkeley, Berkeley, CA, USA, Tech. Rep., 2001.

[30] T. V. Nguyen and M. Kankanhalli, "As-similar-as-possible saliency fusion," *Multimedia Tools Appl.*, vol. 76, no. 8, pp. 10501–10519, Apr. 2017.

[31] L. Mai, Y. Niu, and F. Liu, "Saliency aggregation: A data-driven approach," in *Proc. IEEE Conf. Comput. Vis. Pattern Recognit.*, Jun. 2013, pp. 1131–1138.

[32] M. A. Bagheri, G. Hu, Q. Gao, and S. Escalera, "A framework of multi-classifier fusion for human action recognition," in *Proc. 22nd Int. Conf. Pattern Recognit.*, Aug. 2014, pp. 1260–1265.

[33] B. Fernando, E. Fromont, D. Muselet, and M. Sebban, "Discriminative feature fusion for image classification," in *Proc. IEEE Conf. Comput. Vis. Pattern Recognit.*, Jun. 2012, pp. 3434–3441.

[34] E. Buza, E. Turajlic, and A. Akagic, "Comparative analysis of simple rules for flame recognition," in *Proc. 30th Telecommun. Forum (TELFOR)*, Nov. 2022, pp. 1–4.

[35] R. Soni and B. Mehta, "Diagnosis and prognosis of incipient faults and insulation status for asset management of power transformer using fuzzy logic controller & fuzzy clustering means," *Electr. Power Syst. Res.*, vol. 220, Jul. 2023, Art. no. 109256.

[36] P. Kaur and T. Chaira, "A novel fuzzy approach for segmenting medical images," *Soft Comput.*, vol. 25, no. 5, pp. 3565–3575, Mar. 2021.

[37] X.-X. Yin and S. Hadjiloucas, "Digital filtering techniques using fuzzy-rules based logic control," *J. Imag.*, vol. 9, no. 10, p. 208, Sep. 2023.

[38] N. D. Anh, P. Van Thanh, D. T. Lap, N. T. Khai, T. Van An, T. D. Tan, N. H. An, and D. N. Dinh, "Efficient forest fire detection using rule-based multi-color space and correlation coefficient for application in unmanned aerial vehicles," *Trans. Internet Inf. Syst.*, vol. 16, no. 2, pp. 381–404, 2022.

[39] C. Emmy Prema, S. S. Vinsley, and S. Suresh, "Efficient flame detection based on static and dynamic texture analysis in forest fire detection," *Fire Technol.*, vol. 54, no. 1, pp. 255–288, Jan. 2018.

[40] D. Dzigal, A. Akagic, E. Buza, A. Brdjanin, and N. Dardagan, "Forest fire detection based on color spaces combination," in *Proc. 11th Int. Conf. Electr. Electron. Eng. (ELECO)*, Nov. 2019, pp. 595–599.

[41] O. Le Meur and Z. Liu, "Saliency aggregation: Does unity make strength?" in *Computer Vision—ACCV 2014*, vol. 9006. Springer, 2015, pp. 18–32.

[42] J. Kittler, M. Hatef, R. P. W. Duin, and J. Matas, "On combining classifiers," *IEEE Trans. Pattern Anal. Mach. Intell.*, vol. 20, no. 3, pp. 226–239, Mar. 1998.

[43] A. Lambora, K. Gupta, and K. Chopra, "Genetic algorithm—A literature review," in *Proc. Int. Conf. Mach. Learn., Big Data, Cloud Parallel Comput. (COMITCon)*, Feb. 2019, pp. 380–384.

[44] A. L. Corcoran and S. Sen, "Using real-valued genetic algorithms to evolve rule sets for classification," in *Proc. 1st. IEEE Conf. Evol. Comput.*, Jul. 1994, pp. 120–124.

[45] E. A. Ríos, F. S. Lasheras, A. S. Sánchez, F. Iglesias-Rodríguez, and M. S. Crespo, "Prediction of computer vision syndrome in health personnel by means of genetic algorithms and binary regression trees," *Sensors*, vol. 19, no. 12, p. 2800, Jun. 2019.

[46] A. Dacal-Nieto, E. Vazquez-Fernandez, A. Formella, F. Martin, S. Torres-Guijarro, and H. Gonzalez-Jorge, "A genetic algorithm approach for feature selection in potatoes classification by computer vision," in *Proc. 35th Annu. Conf. IEEE Ind. Electron.*, Nov. 2009, pp. 1955–1960.
[47] C. Aliani, E. Rossi, M. Soliński, P. Francia, A. Lanatà, T. Buchner, and L. Bocchi, "Genetic algorithms for feature selection in the classification of COVID-19 patients," *Bioengineering*, vol. 11, no. 9, p. 952, Sep. 2024.
[48] W. Juan and W. Ping, "Optimization of fuzzy rule based on adaptive genetic algorithm and ant colony algorithm," in *Proc. Int. Conf. Comput. Inf. Sci.*, Dec. 2010, pp. 359–362.
[49] R. Fu, M. A. Al-Absi, A. A. Al-Absi, and H. J. Lee, "A conservation genetic algorithm for optimization of the e-commerce logistics distribution path," in *Proc. 21st Int. Conf. Adv. Commun. Technol. (ICACT)*, Feb. 2019, pp. 558–562.
[50] M. Ebner, "Engineering of computer vision algorithms using evolutionary algorithms," in *Advanced Concepts for Intelligent Vision Systems*, J. Blanc-Talon, W. Philips, D. Popescu, and P. Scheunders, Eds., Berlin, Germany: Springer, 2009, pp. 367–378.
[51] T. Nakane, N. Bold, H. Sun, X. Lu, T. Akashi, and C. Zhang, "Application of evolutionary and swarm optimization in computer vision: A literature survey," *IPSJ Trans. Comput. Vis. Appl.*, vol. 12, no. 1, p. 3, Dec. 2020.
[52] H. Ishibuchi, K. Nozaki, N. Yamamoto, and H. Tanaka, "Selecting fuzzy if-then rules for classification problems using genetic algorithms," *IEEE Trans. Fuzzy Syst.*, vol. 3, no. 3, pp. 260–270, Mar. 1995.
[53] L. C. Jain and L. I. Kuncheva, "Designing classifier fusion systems by genetic algorithms," *IEEE Trans. Evol. Comput.*, vol. 4, no. 4, pp. 327–336, Apr. 2000.
[54] L. I. Kuncheva, *Fuzzy Sets: Fuzzy Classifier Design*. Heidelberg, Germany: Physica, 2000, pp. 79–115.
[55] L. Zadeh, "Fuzzy sets," *Inf. Control*, vol. 8, no. 3, pp. 338–353, 1965.
[56] J. Fodor, "Aggregation functions in fuzzy systems," in *Aspects of Soft Computing, Intelligent Robotics and Control*. Berlin, Germany: Springer, 2009, pp. 25–50.
[57] Y. Yao, "A comparative study of fuzzy sets and rough sets," *Inf. Sci.*, vol. 109, nos. 1–4, pp. 227–242, Aug. 1998.
[58] S. Rahimi, M. Zargham, A. Thakre, and D. Chhillar, "A parallel fuzzy C-mean algorithm for image segmentation," in *Proc. IEEE Annu. Meeting Fuzzy Inf., Process.*, vol. 1, Sep. 2004, pp. 234–237.
[59] R. Katarya and O. P. Verma, "An effective web page recommender system with fuzzy c-mean clustering," *Multimedia Tools Appl.*, vol. 76, no. 20, pp. 21481–21496, Oct. 2017.
[60] I. Perfilieva and B. De Baets, "Fuzzy transforms of monotone functions with application to image compression," *Inf. Sci.*, vol. 180, no. 17, pp. 3304–3315, Sep. 2010.
[61] R. Boukezzoula, S. Galichet, and L. Foulloy, "MIN and MAX operators for fuzzy intervals and their potential use in aggregation operators," *IEEE Trans. Fuzzy Syst.*, vol. 15, no. 6, pp. 1135–1144, Dec. 2007.
[62] H.-J. Zimmermann, "Fuzzy set theory," *WIREs Comput. Statist.*, vol. 2, no. 3, pp. 317–332, 2010.
[63] U. F. Simo and H. Gwét, "Fuzzy triangular aggregation operators," *Int. J. Math. Math. Sci.*, vol. 2018, pp. 1–13, Jan. 2018.
[64] M. Mas, M. Monserrat, J. Torrens, and E. Trillas, "A survey on fuzzy implication functions," *IEEE Trans. Fuzzy Syst.*, vol. 15, no. 6, pp. 1107–1121, Dec. 2007.
[65] T. Toulouse, L. Rossi, A. Campana, T. Celik, and M. A. Akhloufi, "Computer vision for wildfire research: An evolving image dataset for processing and analysis," *Fire Saf. J.*, vol. 92, pp. 188–194, Sep. 2017.
[66] R. Ghali and M. A. Akhloufi, "Deep learning approaches for wildland fires remote sensing: Classification, detection, and segmentation," *Remote Sens.*, vol. 15, no. 7, p. 1821, Mar. 2023.
[67] D. Ogwok and E. M. Ehlers, "Jaccard index in ensemble image segmentation: An approach," in *Proc. 5th Int. Conf. Comput. Intell. Intell. Syst.*, Nov. 2022, pp. 9–14.
[68] N. Otsu, "A threshold selection method from gray-level histograms," *IEEE Trans. Syst., Man, Cybern.*, vol. SMC-9, no. 1, pp. 62–66, Jan. 1979.
[69] P. Hong, L. Chengde, L. Linkai, and Z. Qifeng, "Accuracy of classifier combining based on majority voting," in *Proc. IEEE Int. Conf. Control Autom.*, May 2007, pp. 2654–2658.
[70] A. Kumar, R. Sushil, and A. K. Tiwari, "Classification of breast cancer using user-defined weighted ensemble voting scheme," in *Proc. IEEE Region 10 Conf. (TENCON)*, Dec. 2021, pp. 134–139.
[71] A. Dogan and D. Birant, "A weighted majority voting ensemble approach for classification," in *Proc. 4th Int. Conf. Comput. Sci. Eng. (UBMK)*, Sep. 2019, pp. 1–6.
[72] D. Chicco and G. Jurman, "The advantages of the Matthews correlation coefficient (MCC) over F1 score and accuracy in binary classification evaluation," *BMC Genomics*, vol. 21, no. 1, pp. 1–13, Dec. 2020.
[73] D. Chicco, M. J. Warrens, and G. Jurman, "The Matthews correlation coefficient (MCC) is more informative than Cohen's Kappa and brier score in binary classification assessment," *IEEE Access*, vol. 9, pp. 78368–78381, 2021.
[74] A. Lissovoi and P. S. Oliveto, "Computational complexity analysis of genetic programming," in *Theory of Evolutionary Computation: Recent Developments in Discrete Optimization*. Cham, Switzerland: Springer, 2020, pp. 475–518.
[75] A. Piszcz and T. Soule, "Genetic programming: Optimal population sizes for varying complexity problems," in *Proc. 8th Ann. Conf. Genet. Evol. Comput.*, 2006, pp. 953–954.

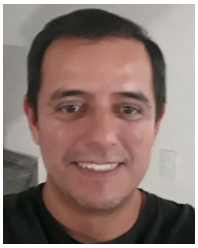

ALBERTO LOPEZ-ALANIS received the M.Eng. degree in electronics from the Universidad Autonoma de Tamaulipas, Mexico, in 2010, and the D.Eng. degree from the Universidad de Guanajuato, in 2019. He is currently a Postdoctoral Researcher for CONACYT with the Center for Research in Mathematics. His current research interests include expert systems, computer vision, and image processing.

HECTOR DE-LA-TORRE-GUTIERREZ received the B.E. degree in statistical industrial engineering from the Autonomous University of Aguascalientes, in 2010, and the Ph.D. degree from the University of Birmingham, in 2017. He is currently an Associate Researcher (Investigador por Mexico) with the Centre for Research in Mathematics, Mexico. His research interests include image processing, computer vision, application of machine learning to natural language processing, statistical modeling, information fusion, and multivariate analysis.

ARTURO HERNÁNDEZ-AGUIRRE received the master's and Ph.D. degrees in computer science from Tulane University, USA, in 2001. He has been a Titular "C" Researcher with the Center for Research in Mathematics, CIMAT, since 2001. He has published nearly 50 journal articles, 20 book chapters, and more than 100 papers in international conferences. His areas of interest are evolutionary algorithms and artificial intelligence. He has been a member of the Technical Council of Science and Technology, Guanajuato. He is a member of the technical council of various specialized magazines and international conferences.

MARÍA T. ORVAÑANOS-GUERRERO received the M.Sc. and D.Eng. degrees from the Universidad Panamericana, Aguascalientes Campus, in 2022. She is currently an Electronics and Digital Systems Engineer with a major in robotics. She is an Associate Professor and the Vice Dean of the Engineering Faculty, Universidad Panamericana. She is a Titular "B" Researcher with the Universidad Panamericana. Her research interests include computer vision, expert systems, mechatronic and dynamics systems, and robotics. She is a member of Mexican Research Systems.